ENVIRONMENTAL RESEARCH
LETTERS

LETTER • OPEN ACCESS

Are there lightning fires in the Brazilian Amazon?

To cite this article: Cunhui Zhang *et al* 2026 *Environ. Res. Lett.* **21** 024025

IOP Publishing Environ. Res. Lett. 21 (2026) 024025 https://doi.org/10.1088/1748-9326/ae3786

ENVIRONMENTAL RESEARCH
LETTERS

Check for updates

OPEN ACCESS

RECEIVED
11 November 2025

REVISED
24 December 2025

ACCEPTED FOR PUBLICATION
13 January 2026

PUBLISHED
27 January 2026

LETTER

Are there lightning fires in the Brazilian Amazon?

Cunhui Zhang[1,*], Thomas A J Janssen[1,2], Jose V Moris[1], Niels Andela[3], Matthew W Jones[4], Renata Libonati[5], Lucas Menezes[5], Imma Oliveras Menor[6], Carlota Segura-Garcia[7] and Sander Veraverbeke[1,4]

[1] Faculty of Science, Vrije Universiteit Amsterdam, De Boelelaan 1100, Amsterdam 1081 HV, The Netherlands
[2] Plant Ecology and Nature Conservation Group, Wageningen University, Droevendaalsesteeg 3a, Wageningen 6708 PB, The Netherlands
[3] BeZero Carbon Ltd, 5 New Street Square, London EC4A 3TW, United Kingdom
[4] School of Environmental Sciences, University of East Anglia (UEA), Norwich Research Park, Norwich NR4 7TJ, United Kingdom
[5] Departamento de Meteorologia, Rio de Janeiro, Universidade Federal do Rio de Janeiro, RJ, Brazil
[6] School of Geography and the Environment, Environmental Change Institute, University of Oxford, Oxford, United Kingdom
[7] Departamento de Geología, Geografía y Medio Ambiente, Universidad de Alcalá, 28801 Alcalá de Henares, Spain
[*] Author to whom any correspondence should be addressed.

E-mail: z.c.h.zhang@vu.nl

Keywords: lightning-ignited fires, anthropogenic fires, natural ignition, fire regime, Amazon rainforest

Supplementary material for this article is available online

Abstract

The Brazilian Amazon contains approximately 40% of the world's tropical rainforest and plays a critical role in preserving biodiversity and regulating water, energy and carbon cycles. However, deforestation and increasingly frequent droughts, heatwaves and wildfires threaten these rainforests. Amazonian fires are generally assumed to be entirely anthropogenic, which has led to lightning-ignited fires being underexplored. Here, we present the first detailed assessment of the spatiotemporal patterns of lightning-ignited fires in the Amazon rainforest to elucidate the role of lightning and human ignitions in shaping Amazon fire dynamics. To do this, we matched cloud-to-ground lightning strokes from the Global Lightning Dataset (GLD360) with individual fire events between 2019 and 2024 to obtain a probability of lightning ignition for each fire. We also calculated a human-ignition probability index using proximity to roads, waterways, and human land cover as proxies for human activity. By combining both probabilistic indices with ground-observed lightning ignitions from eight protected areas, we could optimize the threshold that determines if an ignition is more likely to be caused by lightning or human activities. We estimate that in the Brazilian Amazon, lightning caused on average 0.2%–0.4% of all fires each year (234–407 ignitions per year) and 1.1%–1.2% of the annually burned area (1226–1358 km^2 per year) between 2019 and 2024. More than 89% of these fires occurred in the late dry season between August and November, peaking in September and October. Despite lightning-ignited fires contributing a small proportion of all Amazonian fires, they constitute over 25% of the fires in identified grid clusters in parts of the states of Pará (particularly in the Breves region), Amazonas, and Rondônia. This study provides the first estimation of the role of natural ignitions in Amazon fire dynamics and a scientific basis for understanding their contribution within the region.

1. Introduction

The Amazon accounts for 40% of the global tropical forest area, making it the largest tropical forest in the world (Laurance *et al* 2001, Aragão *et al* 2014). It is a vital component of the global carbon cycle and a biodiversity hotspot that harbors millions of species (Cardoso *et al* 2017). In addition, the Amazon plays a crucial role in regulating the global climate as it is an important driver of global water, carbon and energy cycles (Sampaio *et al* 2007, Spracklen and Garcia-Carreras 2015, Nobre *et al* 2016).

The Amazon forest typically maintains high moisture levels in both the soil and the litter layer throughout the year (Leigh 1975). The dense and complex canopy further contributes to preserving a microclimate with high atmospheric humidity, making fire occurrence relatively rare (Kapos 1989, Uhl and

Kauffman 1990a). Even when fires occur, their ecological impact is usually limited, because canopy–atmosphere decoupling sustains a humidity microclimate (Ray *et al* 2005). However, droughts and heatwaves have become more frequent and more severe in Amazonia in the last decades resulting from intensifying climate change and amplified by large-scale climate modes such as El Niño Southern Oscillation (ENSO) and the Atlantic Multidecadal Oscillation (AMO), alongside reduced regional moisture recycling resulting from large-scale deforestation (Khanna *et al* 2017, Janssen *et al* 2020, Libonati *et al* 2022). Furthermore, forest degradation and fragmentation also directly promote fire occurrence by creating more forest edge where vegetation is directly exposed to sunlight and can desiccate, though fires rarely spread into the intact forest interior (Lapola 2023). During prolonged drought, leaf litterfall increases substantially in the Amazon, contributing to rare dry surface fuels (Janssen *et al* 2021). Furthermore, during prolonged drought even typically interior fuels can dry out and become flammable, allowing ignitions to potentially trigger large wildfires (Cochrane 2003, Brando *et al* 2019). Despite their lower fire occurrence, tropical humid forest and rainforest vegetation are relatively vulnerable to fire because many tree species did not co-evolve with fire, lacking fire-adaptive traits such as thick bark and resprouting (Pivello *et al* 2021). This makes rainforest tree species suffer much higher mortality rates from fires compared to fire-adapted tree species from savanna and tropical dry forest ecosystems (Uhl and Kauffman 1990a, Bush *et al* 2011, Hendricks *et al* 2024).

During the pre-Columbian period (before 1492 CE), Amazonian forest fires are estimated to have recurred only once every 400–1000 years, mainly during rare extreme droughts associated with exceptional ENSO events (Thonicke *et al* 2001, Bush *et al* 2008, Alencar *et al* 2015). However, fire frequency in the Amazon region has been substantially higher in recent decades, mainly because of deforestation, agricultural expansion and forest degradation (Schmidt and Eloy 2020, Libonati *et al* 2021, Silveira *et al* 2022, Flores *et al* 2024). Furthermore, fire risk has been exacerbated by climate change-induced droughts and heatwaves (Marengo *et al* 2018, Costa *et al* 2022, Libonati *et al* 2022), often amplified by large–scale modes of climate variability such as ENSO and AMO (Jiménez-Muñoz *et al* 2016, Zhao *et al* 2018, Singh *et al* 2022).

Fires are ignited either by humans or by natural phenomena, which is almost exclusively lightning (Janssen *et al* 2023). The Brazilian Amazon experiences some of the highest lightning activity globally (Pinto and Pinto 2003), with potentially large effects on tree mortality and biomass stocks (Almeida *et al* 2012, Gora *et al* 2025, Veraverbeke *et al* 2025). Although studies have examined the impact of lightning strokes on tropical tree mortality and damage (Yanoviak *et al* 2020, Gora *et al* 2020a, 2020b), no studies have formally quantified their role in fire ignitions in tropical forests. Addressing this gap is essential for better understanding Amazon fire regimes, including the role of natural fires in these ecosystems, such as their dynamics, frequency, drivers, risks and carbon emissions.

This study presents the first comprehensive analysis of lightning fires throughout the entire Brazilian Amazon rainforest. We used a global lightning network dataset and remotely sensed fire data between 2019 and 2024. First, we evaluated the temporal and spatial concurrence of lightning strokes and fire ignition events to estimate a probability-based index of lightning fire ignitions. Second, we calculated a similar ignition probability but then resulting from human activities by evaluating nearby land use and infrastructure. We assessed the uncertainty in our attribution by comparing the probability indices of lightning and human fires using officially recorded ground-based fire cause data. This allowed us to map and understand the spatiotemporal patterns of lightning fires in the Brazilian Amazon rainforest.

2. Materials and methods

2.1. Study area

Our study focuses on the Brazilian Amazon in South America (figure 1), which covers approximately 4.0 million km^2 (Souza *et al* 2020). This represents about 60% of the Amazon rainforest's total estimated 6.7 million km^2 (Aragão *et al* 2014). The region's vast size contributes to considerable climate variability across the basin with a relatively long dry season of up to six months (defined as months with less than 100 mm of precipitation) in the south-east and no dry season in the north-west (Sombroek 2001). However, the climate is generally warm and humid resulting in intense convective activity, modulated by the influence of synoptic systems (Moura *et al* 2019, da Silva *et al* 2023). Consequently, annual rainfall generally falls between 2000 mm and 2500 mm, supplied by the South Atlantic Ocean and regional recycling of evapotranspiration (Moura *et al* 2019, Marengo *et al* 2024). Mean annual temperatures range from 25.0 °C to 27.8 °C (Almeida *et al* 2017). Rising temperatures and increasingly frequent droughts associated with climate change have recently intensified fire-conducive conditions during the dry season months, increasing the region's vulnerability to wildfires (Feron *et al* 2024, Flores *et al* 2024).

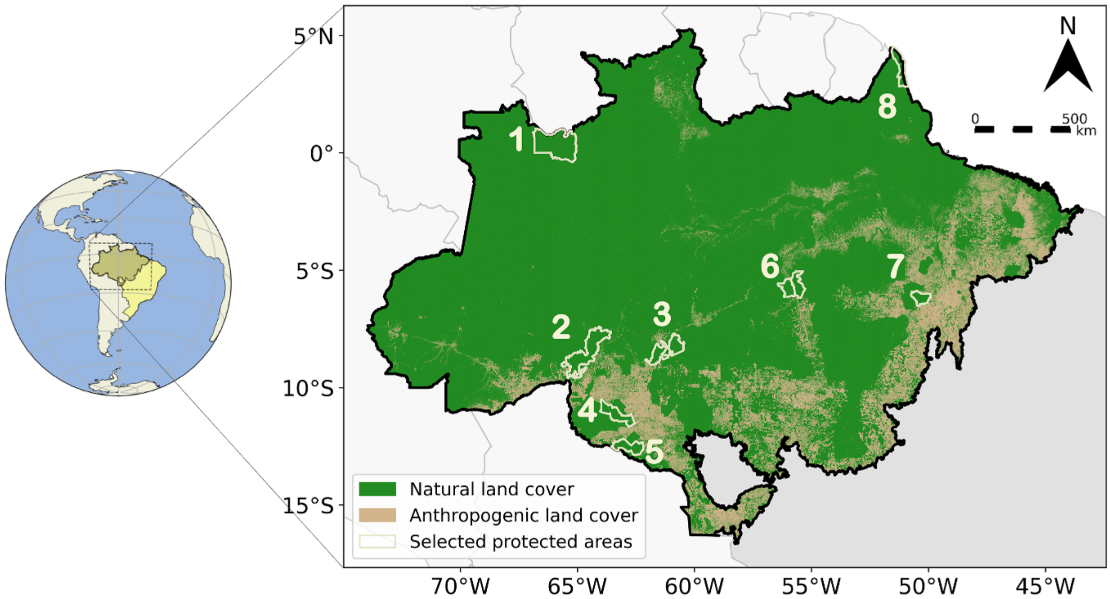

Figure 1. Location of the Brazilian Amazon (black polygon) in South America. The green and brown areas represent natural and anthropogenic land cover respectively, based on MapBiomas Collection 9 land cover data (MapBiomas Project 2024). The white polygons represent eight selected protected areas where ground-based fire cause data were available, with numbers indicating the corresponding protected area labels according to Table 1.

2.2. Datasets

2.2.1. Remotely sensed fire data

We used the fire event dataset from the Amazon Fire Dashboard (AFD). The AFD is a comprehensive resource that clusters Visible Infrared Imaging Radiometer Suite (VIIRS) active fire detections (Schroeder *et al* 2014) into individual fire events using a near-real time fire tracking methodology (Andela *et al* 2022). In this dataset, each event is classified into four fire types typical for the Amazon: deforestation fire, understory forest fire, small clearing and agricultural fire, and savanna fire. To provide an assessment that is independent from the AFD fire type classification, we included all fires detected within the AFD. The dataset provides detailed information for each fire event, including data on event start day, duration, tree cover, vegetation biomass, historical deforestation rates, fire radiative power, size, fire polygon geometry, etc.

Accurate attribution of fire ignitions requires assessing the temporal and spatial coherence of lightning and fire events. Although the AFD is comprehensive in coverage, it provides fire detections at a daily temporal resolution, posing challenges for temporal matching with lightning strokes, which have a sub-second temporal resolution. To address this limitation, we integrated AFD fire event data with the native temporal resolution of VIIRS active fire data, which provides data twice per day, to provide a more accurate timestamp of the first fire detection (defined as ignition time).

For the integration, we used the 375 m VIIRS active fire product (level 2, VNP14IMG) derived from both the Suomi National Polar-orbiting Partnership and National Oceanic and Atmospheric Administration-20 (NOAA-20) platforms (Schroeder *et al* 2014). This dataset includes the time of active fire detection, geolocation and fire radiative power. For each AFD fire polygon, we identified the earliest VIIRS active fire detection within the polygon. Often, multiple VIIRS fire detections were selected as the earliest fire detection, as the earliest observations covered multiple VIIRS pixels. To estimate the location of the fire ignition for each AFD fire polygon, we created a buffer with a 375 m radius around all the active fire detections selected for that polygon. In such a manner, for each AFD fire polygon, we delineated the minimum bounding rectangle containing the buffers of the earliest VIIRS detections. This VIIRS-based rectangle was defined as the area of ignition (AoI) and represents the smallest area where the ignition could have taken place. The centroid of the AoI was used as a reference ignition point.

2.2.2. Lightning data

The Vaisala Global Lightning Dataset (GLD360) is derived from a global network of ground-based sensors that detect very low frequency (VLF) radio waves emitted by lightning in real time (Cummins *et al* 1998, Said *et al* 2010). GLD360 predominantly detects cloud-to-ground (CG) lightning strokes and also captures some intra-cloud flashes. Between 2019 and 2024, over 200 million (205 781 952) CG strokes were recorded within the study area (figure 2). Of this grand total, about 84 million (84 292 890) CG strokes were matched to fire ignitions because of spatial and temporal proximity (see section 2.3.1. For additional details). CG lightning stroke density between 2019

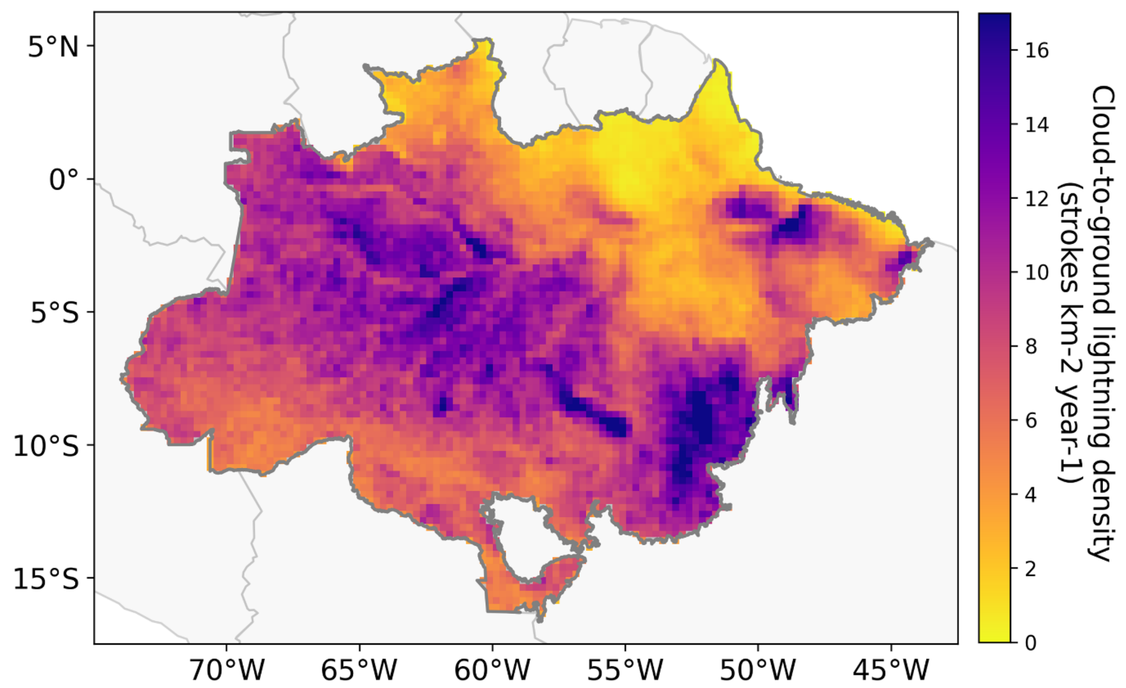

Figure 2. Average annual cloud-to-ground lightning stroke density over the Brazilian Amazon. Data are derived from the Global Lightning Dataset (GLD360) and were detected between 2019 and 2024. Cloud-to-ground lightning events were spatially aggregated to a 0.25° regular grid.

and 2024 was significantly higher in the southwestern Amazon than in the northeast (figure 2). In the southwest, moisture–laden convection driven by regional monsoon dynamics and substantial moisture recycling leads to vigorous thunderstorms. In contrast, the northeast receives most of its precipitation as more stable, stratiform Atlantic-dominated rainfall, resulting in much lower lightning activity (Yoon and Zeng 2010). The GLD360 dataset provides the location, timestamp, polarity and amplitude of each CG stroke, along with its spatial uncertainty, represented by a 50% confidence ellipse defined by its orientation angle and the lengths of the semi-major and semi-minor axes.

2.2.3. Land cover and infrastructure data

To estimate the likelihood of human fire ignitions, we compared the fractions of natural and human-modified land cover types in the vicinity of each fire ignition location. We used land cover information from 2019 to 2024 from the annual land cover maps of Brazil produced by the MapBiomas Project (Collection 9, 2023) (Souza *et al* 2020, MapBiomas Project 2024). This land cover data, with a spatial resolution of 30 m, provides predefined natural and anthropogenic land cover types (table S1). The class labeled as 'Not Observed' was excluded from the analysis. We created a circular buffer with a 0.01° (approximately 1 km) radius surrounding each ignition centroid and then calculated the fractions of natural and human-modified land cover within the buffer. To further evaluate the proximity of ignitions to human activity, we used data on roads, waterways, villages, and powerlines from OpenStreetMap (OpenStreetMap 2021) and the 'Departamento Nacional de Transportes' (the Brazilian National Transport Department 2024), (figure S1).

2.2.4. Meteorological data

To characterize the weather conditions at the time of fire ignition, we analyzed precipitation and vapor pressure deficit (VPD). We obtained hourly total precipitation, 2 m air temperature and dewpoint temperature data at 0.1° spatial resolution from the fifth generation of the European Centre for Medium-Range Weather Forecast (ECMWF) reanalysis (ERA5-Land) dataset (Muñoz-Sabater *et al* 2021). We extracted total daily precipitation and hourly VPD values surrounding each fire ignition day. VPD was calculated from hourly air temperature and dewpoint temperature using Tetens equation following Monteith and Unsworth (Otto Tetens 1930, Monteith and Unsworth 2013). We also computed the total precipitation accumulated over the five days preceding the ignition date. From the hourly VPD, we calculated the daily average and maximum VPD over the same 5 d period, to capture variability in atmospheric aridity.

2.2.5. Ground reference data on fire cause

We used reference data from eight protected areas in the Brazilian Amazon for our lightning ignition attribution calibration (figure 1). This data was documented by the 'Instituto Chico Mendes de

Conservação da Biodiversidade' (ICMBio), the federal agency responsible for managing and protecting Brazil's conservation units and biodiversity (ICMBio 2025). The ICMBio dataset provides ground-verified fire records, including precise ignition locations, dates and documented causes based on visual confirmation. The ICMBio dataset documents 20 visually confirmed lightning-ignited fire events recorded between 2019 and 2023 across the eight protected areas. When cross-referenced with the AFD fire dataset from the same period, seven of these fires were successfully matched to AFD lightning fire events, while the remaining 13 had no corresponding record in the AFD. In addition, 892 other fire events detected by AFD within these protected areas during 2019–2023 showed no indication of lightning ignition in the ICMBio records and were therefore assumed to be anthropogenic in origin (table 1).

2.3. Methods

2.3.1. Lightning ignition probability

The relationship between CG lightning and fire ignitions between 2019 and 2024 was investigated using spatio-temporal probability matching (Moris *et al* 2024b). This approach introduces a probabilistic index (P_m) to determine the probability that lightning stroke ignited a wildfire, which is the product of a spatial probability (P_s) and a temporal probability (P_t). In this method, a spatial bivariate Gaussian distribution is constructed for each CG stroke using the recorded stroke location and the confidence ellipse parameters. The obtained probability density function is then integrated over the (AoI, section 2.2.1) to compute the spatial probability (P_s) of lightning stroke occurrence within the AoI (Moris *et al* 2024b). Subsequently, the temporal probability (P_t) was calculated for each stroke, which is based on the temporal proximity between the lightning stroke and the ignition. After initial lightning ignition, fires can smolder undetected and it can take up to several days before the fire develops into a flaming fire detectable by satellite sensors such as VIIRS (Moris *et al* 2023). This period between lightning stroke detection and first fire detection is called holdover time. We set the maximum holdover at seven days, as the occurrence of lightning-ignited fires beyond this period is assumed to be minimal. Moris *et al* (2024a) developed survival functions to compute the temporal probability P_t. While specific survival functions are currently available for three biomes (boreal, temperate coniferous forests, and Mediterranean ecosystems), this is not the case for tropical forests, and hence we used a general survival function (parameters: shape = 0.369 and rate = 0.235) that can be applied to other biomes (Moris *et al* 2024a). The probability index P_m quantifies the likelihood that a single CG stroke ignited a particular wildfire by multiplying the spatial and temporal probabilities:

$$P_m = P_s \times P_t. \tag{1}$$

In this study, we calculated the lightning ignition probability for all CG strokes within a 10 km buffer around the AoI, which is a common distance used in fire-lightning matching studies and accounts for potential large location errors in both fire and lightning data (Moris *et al* 2020). Among these strokes, we selected the one with the highest P_m value as the most likely candidate lightning stroke responsible for the ignition. Finally, for each fire, we computed the probability that the ignition was caused by lightning (P_l) by using the inclusion–exclusion principle on the P_m values of all lightning strokes matched to the ignition (Larjavaara *et al* 2005, Menezes *et al* 2022):

$$P_l = 1 - \left(\prod_{i=1}^{n} 1 - P_{m,i}\right). \tag{2}$$

2.3.2. Anthropogenic ignition probability

Given the high frequency of lightning in the Amazon, a large number of CG strokes may spatially and temporally overlap fire ignition areas purely by chance. To minimize lightning ignition commission errors, we also calculated a probability index of anthropogenic fire ignition (P_a). To analyze the spatial distribution of fire ignitions relative to human activities, we first calculated the shortest distance from each ignition location to the nearest anthropogenic feature, including infrastructure, transport waterways, built-up areas, roads, villages and powerlines. We aggregated fire ignition numbers per distance class to construct the raw ignition distribution, which shows an exponential decline in ignitions with increasing distance to anthropogenic features (figure S2(a)). However, this decline can be largely attributed to the distribution of land area rather than human influence as more land area (in km^2) is close to anthropogenic features and less land area is far away from them, showing a similar exponential decline (figure S2(a)). To remove the spatial bias, we calculated the ignition density as the total number of ignitions divided by the total land area within each distance class. To do this, the geospatial features were rasterized into 30 m resolution grids, and proximity distances were calculated for each grid cell. We then fitted an exponential decay model to the normalized ignition density distribution to derive an anthropogenic ignition probability based on distance to human activity and accessibility features (P_r) for each fire event (figure S2(b)). The rationale behind this method is that the spatial distribution in lightning ignitions is assumed to be largely independent

Table 1. Number of lightning-ignited and anthropogenic fire events in eight protected areas of the Brazilian Amazon between 2019 and 2023. Values are reported as the number of lightning-ignited fires/the number of anthropogenic fires. ID numbers correspond to the protected area locations shown in figure 1.

ID	Protected area	Lightning/anthropogenic fires 2019	2020	2021	2022	2023	Total
1	Parque Nacional do Pico da Neblina	0/17	0/14	0/9	0/11	0/12	0/63
2	Parque Nacional Mapinguari	3/16	1/24	0/34	1/35	0/27	5/136
3	Parque Nacional dos Campos Amazônicos	0/40	0/41	0/45	0/40	0/43	0/209
4	Parque Nacional de Pacaás Novos	0/15	0/15	0/6	0/14	1/ 8	1/68
5	Reserva Biológica do Guaporé	0/23	0/61	0/50	0/28	0/61	0/223
6	Parque Nacional do Jamanxim	0/24	0/34	0/16	0/24	0/36	0/124
7	Floresta Nacional de Carajás	0/0	0/21	0/2	0/1	0/0	0/24
8	Parque Nacional do Cabo Orange	0/9	0/1	1/4	0/4	0/27	1/45
	Total	3/144	1/211	1/166	1/157	1/214	**7/892**

of anthropogenic features while human ignitions are strongly dependent on the proximity to anthropogenic features. In addition, we used the MapBiomas land use dataset with two predefined categories, natural and human-modified land (table S1), and calculated the fraction of each land cover type within a 0.01° (approximately 1 km) radius buffer around the ignition centroid (P_{hl}). Based on the inclusion–exclusion principle (Dorph *et al* 2022), we calculated a probability index of anthropogenic fires (P_{a}) as follows:

$$P_{\mathrm{a}} = 1 - (1 - P_{\mathrm{r}}) \times (1 - P_{\mathrm{hl}}) \quad (3)$$

where P_{r} is the probability based on the shortest distance between ignition centroids and human or accessibility features, and P_{hl} is the proportion of human land cover within the buffer zone around the ignition centroid.

2.3.3. Uncertainty analysis

In our ignition attribution framework, ignitions can exhibit both high lightning and high anthropogenic probability index values. This is the case, for example, when an ignition is located next to a road while also being matched to multiple co-occurring lightning strokes. Because the two probability indices are derived from different methodologies and datasets, they cannot be directly compared and do not share a common scale, even though both range from zero to one. To enable confident attribution of ignitions, we defined a probability difference index (Δ_p) between the two probability indices. This index (Δ_p) was subsequently used for calibration against the reference data described in the section 2.2.5.:

$$\Delta_p = P_{\mathrm{l}} - P_{\mathrm{a}}. \quad (4)$$

We performed best threshold (BT) selection to maximize the detection of relatively rare lightning ignitions while minimizing overall misclassification. We also conducted an uncertainty range (Δ_t) analysis to provide a measure of attribution uncertainty and enhance the robustness of the results. The ground reference data from eight protected areas within the Brazilian Amazon were labeled as true observed data, while different thresholds of Δ_p values served as predicted classifications. This approach resulted in four possible classifications:

- True positive (TP): a fire actually caused by lightning is correctly identified.
- False negative (FN): a fire actually caused by lightning is incorrectly identified as human-caused.
- True negative (TN): a fire actually caused by human activity is correctly identified.
- False positive (FP): a fire actually caused by human activity is incorrectly identified as lightning-caused.

We used the receiver operating characteristics (ROC) curve (Fawcett 2006) to characterize the ability to differentiate between TP rates (TPRs) and FP rates (FPRs) (equation (5) and (6)). ROC curves have FPR on the horizontal axis and TPR on the vertical axis, and the ideal point is (0, 1), which would mean that the ability to differentiate between both fire causes is correctly assessed in all cases (figure S3(a)),

$$\mathrm{TPR} = \frac{\mathrm{TP}}{\mathrm{TP} + \mathrm{FN}} \quad (5)$$

$$\mathrm{FPR} = \frac{\mathrm{FP}}{\mathrm{FP} + \mathrm{TN}}. \quad (6)$$

We calculated FPRs, TPRs and their corresponding Δ_p thresholds along the ROC curve. The BT was selected by identifying the Δ_p threshold with the shortest distance to the ideal point on the ROC curve, as given by equation (7). To obtain the optimal Δ_t, we first examined the performance of adjacent thresholds around the BT to determine the first uncertainty range Δ_{t1} (figure S3(b)). Additionally, we employed a bootstrap method (DiCiccio and Efron 1996) to randomly resample the calculated set of FPRs, TPRs, and Δ_p thresholds 1000 times, generating several ROC curves and corresponding BTs. We obtained the second uncertainty range Δ_{t2} by analyzing the distribution of the BTs across all resampling results and using the 95% confidence interval. By taking the intersection of these two ranges, we defined the uncertainty range Δ_t (equation (8)),

$$\text{Distance} = \sqrt{\text{FPR}^2 + (1 - \text{TPR})^2} \tag{7}$$

$$\Delta_t = \Delta_{t1} \cap \Delta_{t2}. \tag{8}$$

In this study, the BT was $\Delta_p = -0.012$, with an uncertainty range between -0.012 and 0.004. The lower bound of the uncertainty threshold was the same as the optimal value due to the limited number of reference data points. The obtained BT range around zero indicates that, despite using different data and methodologies to obtain the two probabilistic indices, they remain closely comparable. We applied this BT and Δ_t to the reference data and all the remotely sensed fire events to attribute these ignitions to either lightning strokes or human activities (table 2, figure S4). The upper bound threshold may help reduce commission errors by limiting the number of fires classified as lightning-caused, but it may also result in some lightning ignitions being incorrectly attributed to human activities.

3. Results

3.1. Spatiotemporal patterns of different fire causes

We estimate that lightning-ignited fires accounted for 0.4% (uncertainty range: 0.2%–0.4%) of all fires (234–407 ignitions per year) in the Brazilian Amazon between 2019 and 2024, while the corresponding burned area was 1.3% (uncertainty range: 1.1%–1.3%) of the total burned area (1226–1358 km² per year). As expected, human activities were the dominant cause of fire ignitions in the Brazilian Amazon, accounting for 99.6% of the ignitions and 98.7% of the burned area. Although lightning was generally a minor source of fire ignition, lightning-ignited fires showed distinct spatial patterns. Gridded clusters of a higher (>25%) lightning fire contribution were visible across the Brazilian Amazon in the states of Pará (specifically in the Breves region), Amazonas, and Rondônia (figures 3, S5 and S6). These areas also accounted for 90.6% of the total burned area attributed to lightning (figure 3(b)). Conversely, lightning fire activity and associated burned areas were relatively sparse in the northern part of the Brazilian Amazon.

Between 2019 and 2024, the annual number of human ignitions averaged approximately 100 000 events per year (figure 4(a)). In contrast, lightning ignitions were comparatively rare, with an average of approximately 400 ignitions per year (table 2). The lowest number of lightning ignitions was observed in 2022 (288 of the total 107 407 ignitions), compared to the highest number of 558 (of a total 107 479 ignitions) in 2024. Lightning activity in the Amazon peaks between September and December (figure 4(b)), at the end of the dry season and beginning of the wet season for most regions within the Amazon Basin. This lightning seasonality is partly mirrored by the seasonal variation of lightning-ignited fires, which peaks in September–October (figure 4(d)). Compared with anthropogenic fires, lightning fires in the region tend to occur within a narrower seasonal window, despite both showing comparable seasonal dynamics.

To verify whether the regional-scale patterns observed across the entire study area were consistent across different latitudinal zones, we divided the region into four latitudinal bands (figure S7). In the southern hemisphere zones, both anthropogenic and lightning-ignited fire exhibited similar seasonal dynamics, with most fires occurring between August and November. Human-ignited fires typically started in June, while lightning-ignited fires tended to occur later in July. In the northern hemisphere zones, anthropogenic fires exhibited a bimodal seasonal pattern, with distinct peaks in March and October. In contrast, lightning-ignited fires occurred in very limited numbers, yet they also follow a comparable seasonal pattern.

3.2. Fire drivers and impacts

We find that the average VPD for both human-ignited and lightning-ignited fires generally increases during the five days preceding fire detection, reaching a peak on the first day of fire detection (figure 5(a)). VPD associated with human ignitions was on average higher than that for lightning ignitions. A similar pattern is observed in the precipitation analysis, where median and mean cumulative precipitation in the five days before fire detection is generally lower for human ignitions than for lightning ignitions, but the difference on the ignition day is not statistically significant (figure 5(b)). These results suggest that lightning ignitions generally occur under wetter conditions compared to human ignitions, likely because lightning can co-occur with substantial rainfall during thunderstorms. Mean VPD and mean monthly lightning ignition counts show a strong exponential relationship (figure 5(c)), indicating that the probability of lightning ignition occurrence increases exponentially with drier atmospheric conditions. The months September and October showed on average the highest monthly VPD and the highest lightning fire occurrence (figure 5(c)). For lightning ignitions, daily average VPD reached the lowest value three days before first fire detection (figure 5(a)). This temporal pattern is consistent with the peak in holdover time of three days (figure S8), suggesting that many lightning fires in the Amazon are ignited under relatively wet

Table 2. Fire classification accuracy in eight protected areas of the Brazilian Amazon, and estimated number of lightning-ignited fires and their burned area across the entire study region between 2019 and 2024 under different classification thresholds (Δ_p).

<table>
<tr><th>Scenario</th><th colspan="2">Metric/category</th><th>Uncertainty lower bound (and best threshold) $\Delta_p = -0.012$</th><th>Uncertainty upper bound $\Delta_p = 0.004$</th></tr>
<tr><td>Protected areas</td><td colspan="2">Total ignitions</td><td>899</td><td>899</td></tr>
<tr><td></td><td colspan="2">Predicted positive</td><td>127</td><td>65</td></tr>
<tr><td></td><td colspan="2">Predicted negative</td><td>772</td><td>834</td></tr>
<tr><td></td><td colspan="2">Positive</td><td>7</td><td>7</td></tr>
<tr><td></td><td colspan="2">Negative</td><td>892</td><td>892</td></tr>
<tr><td></td><td colspan="2">True positive</td><td>5</td><td>4</td></tr>
<tr><td></td><td colspan="2">True negative</td><td>770</td><td>831</td></tr>
<tr><td></td><td colspan="2">False positive</td><td>122</td><td>61</td></tr>
<tr><td></td><td colspan="2">False negative</td><td>2</td><td>3</td></tr>
<tr><td></td><td colspan="2">True positive rate</td><td>71.4%</td><td>57.1%</td></tr>
<tr><td></td><td colspan="2">False positive rate</td><td>13.7%</td><td>6.8%</td></tr>
<tr><td></td><td colspan="2">Precision</td><td>3.9%</td><td>6.2%</td></tr>
<tr><td></td><td colspan="2">Accuracy</td><td>86.3%</td><td>93.0%</td></tr>
<tr><td>Entire region</td><td>Total</td><td>Ignitions</td><td colspan="2">638 525</td></tr>
<tr><td></td><td></td><td>Burned area</td><td colspan="2">639 779 km^2</td></tr>
<tr><td></td><td>Annual average</td><td>Lightning fire ignitions</td><td>407 (0.4%)</td><td>234 (0.2%)</td></tr>
<tr><td></td><td></td><td>Burned area from lightning fires</td><td>1358 km^2 (1.3%)</td><td>1226 km^2 (1.1%)</td></tr>
</table>

conditions during thunderstorms, after which they smolder for a few days before emerging as flaming fires when weather conditions become drier.

Furthermore, to compare environmental conditions associated with different lightning stroke outcomes, we used a random 1% subsample ($n = 842\,929$) of the matched CG strokes. This sample included both fire-igniting and non-igniting strokes, with the igniting strokes representing a much smaller fraction (0.5%), consistent with the high lightning stroke count and inherent rarity of lightning fire ignitions. Fire-igniting strokes were generally preceded by higher VPD values, indicating drier conditions, and experienced slightly less precipitation on the day of occurrence compared to strokes not resulting in fire ignition (figure S9).

We found that the distributions of the individual fire metrics (fire size, carbon emissions, and fire radiative power) differed markedly between the two fire types (figure 6). These differences were quantified by the power-law exponent β (figure 6, Xu *et al* 2022), which describes the relative frequency of large versus small fires. Higher β values indicate that smaller fires dominate the overall frequency, whereas extremely large-scale events are comparatively rare. Lightning-ignited fires exhibited significantly smaller β values than human-ignited fires across all three impact metrics. This was particularly the case for fire size, showing that rare, high-impact events disproportionately shape the lightning fire regime in the Brazilian Amazon. This relatively small β value of 1.91 further suggests that within the lightning fire distribution, large events constitute a relatively higher proportion of all lightning fires. Consequently, although lightning fires are fewer overall, larger lightning fires dominate their total burned area and carbon emissions, and high fire radiative power events are more frequent for lightning fires compared to anthropogenic fires.

4. Discussion

4.1. Lightning and anthropogenic fires in the Brazilian Amazon

Lightning-ignited fires in the Brazilian Amazon have been largely overlooked because most documented fires in the region have been attributed to human causes. Our analysis shows that lightning fires do occur annually in the Brazilian Amazon, although they comprise a small fraction (0.4%) of all remotely sensed fires between 2019 and 2024. Using ground observations of confirmed lightning ignitions from eight protected areas within the Brazilian Amazon, we optimized our matching algorithm and provided the first estimate of the number of lightning ignitions and their spatial and temporal distribution across this vast area. These ignitions are most common in Pará, Amazonas, and Rondônia states (figure 3), which are to a large extent covered by remote tropical forest with relatively little human activity. However, also in less remote regions with human-dominated fire regimes, we found that a small portion of ignitions can be attributed to lightning. Most areas within the Brazilian Amazon therefore experience

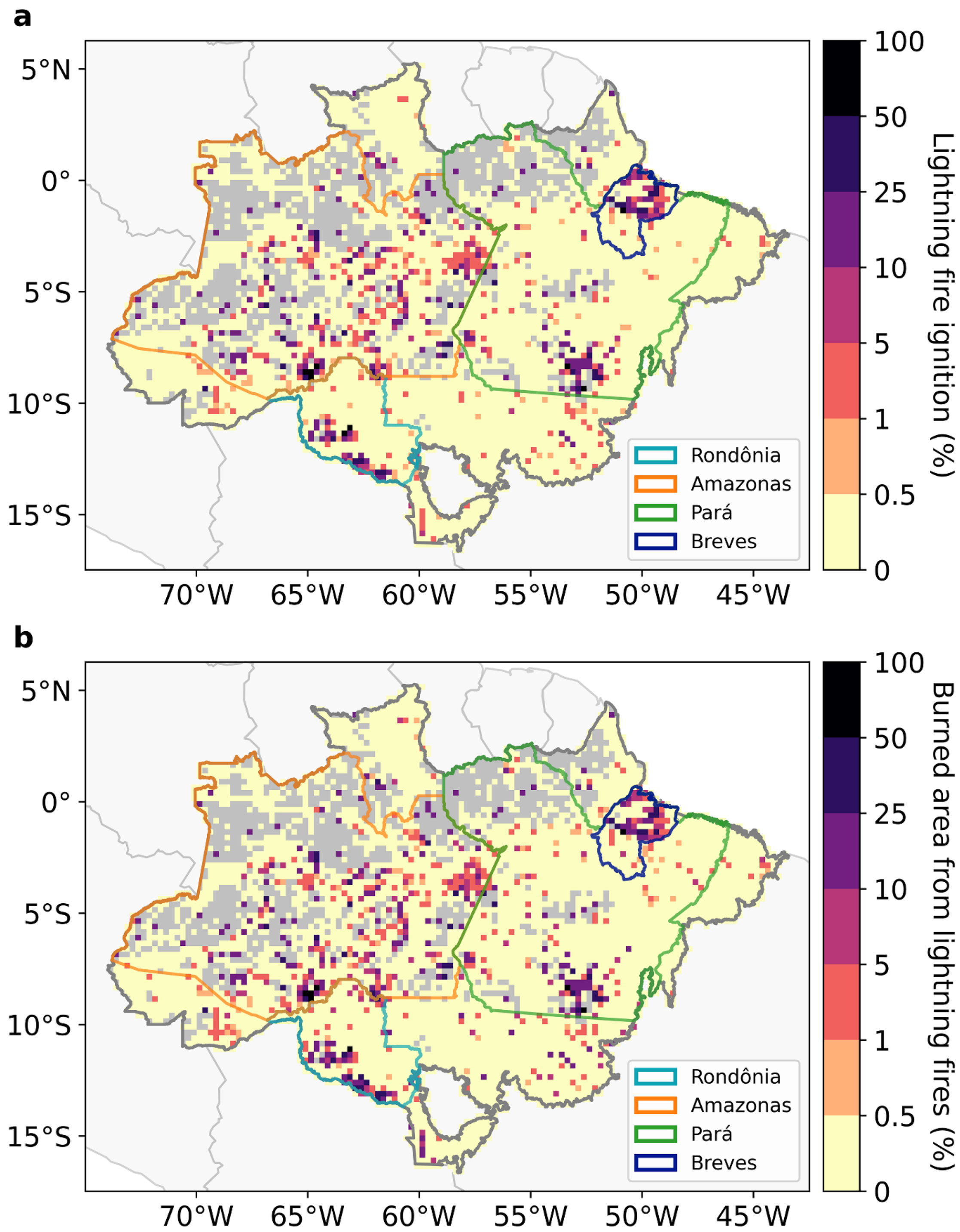

Figure 3. The spatial distribution of lightning-ignited fires using the best threshold (Δ_p) in the Brazilian Amazon (2019–2024). Panel (a) shows the mean annual percentage of lightning fire ignitions and panel (b) shows the associated burned area. Areas without fire occurrence are displayed in dark gray. All fire ignition locations were spatially aggregated to a 0.25° regular grid. Polygons indicate administrative regions where lightning fires were frequently observed (Instituto Brasileiro de Geografia e Estatística—IBGE 2024).

both human-ignited and lightning-ignited fires. We also found that lightning and human ignitions exhibit similar seasonal patterns, generally peaking in the dry season (September–October), although the precise timing differed between climatic zones within the extensive Brazilian Amazon region (figure S7). The spatio-temporal alignment of lightning and human ignitions points to their shared environmental drivers, such as increased soil and atmospheric drought conditions, vegetation desiccation, and fuel accumulation (Longo *et al* 2025, Moreira *et al* 2025).

In our analysis, we estimated the probability of an ignition being caused by human activities using nearby human land cover and the proximity to human infrastructure. However, human activities may also indirectly increase the

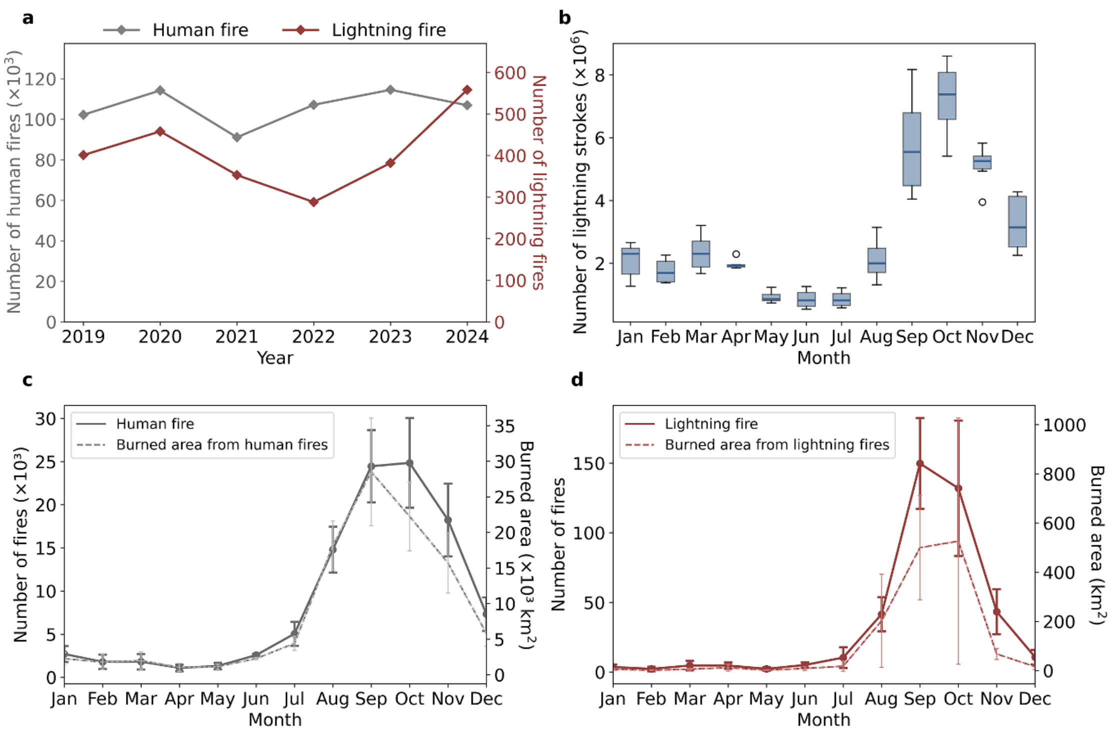

Figure 4. (a) Number of anthropogenic and lightning fires per year between 2019 and 2024. (b) Monthly distribution of cloud-to-ground lightning strokes in the study area over the same period; boxplots represent interannual variation. (c) Seasonal variation in the number of anthropogenic fires and corresponding burned area from 2019 to 2024. (d) Seasonal variation in the number of lightning-ignited fires and their burned area. Error bars in panels (c) and (d) represent the standard deviation; dark line indicate the number of fires and dashed lines indicate burned area.

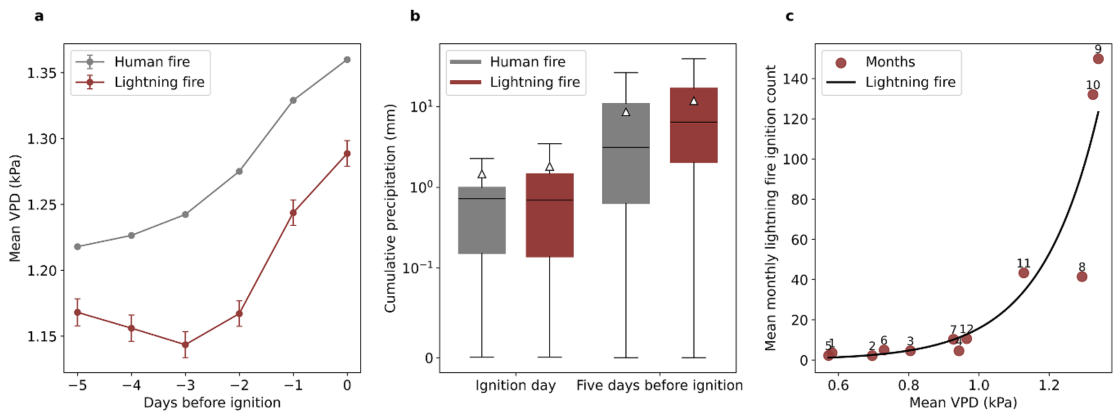

Figure 5. Meteorological conditions surrounding lightning- and human fire ignitions in the Brazilian Amazon. (a) Mean daily vapor pressure deficit (VPD) five days before to the day of the ignition. Error bars indicate the standard error of the mean VPD. (b) Distribution of precipitation on the day of fire and cumulative precipitation in the previous five days, with triangles indicating the mean values. (c) Relationship between mean monthly lightning fire ignition counts and mean VPD across the study period, fitted using the Poisson generalized linear model ($R^2 = 0.92$). Red circles denote the observed monthly values, with numbers indicating the corresponding months; the black line represents the fitted curve.

probability of lightning fire occurrence and its impact. Deforestation and forest degradation not only directly reduce vegetation cover but also result in indirect impacts on fuel loads and microclimate. A decline in canopy cover leads to increased solar radiation reaching the forest floor, increasing surface air temperatures and VPD during the day, drying out the previously humid forest floor and making surface fuels more flammable (Liu *et al* 2025). Furthermore, forest degradation and logging in the Amazon result in an increase of surface fuels, both in the form of woody debris (Keller *et al* 2004) as well as grass encroachment (Brando *et al* 2014). These changes in microclimate and fuel availability significantly increase the probability of fire ignition and spread. Additionally, fires associated with agricultural

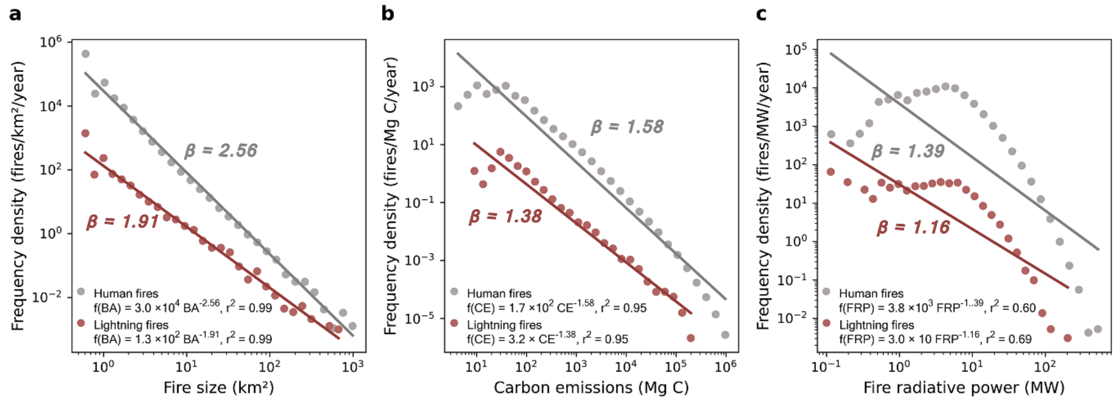

Figure 6. Distribution of (a) fire size (burned area), (b) carbon emissions and (c) fire radiative power for human-ignited fires (gray) and lightning-ignited fires (red) between 2019 and 2024. Circles represent frequency densities $f(x)$, defined as the number of fires per unit bin (1 km^2 for fire size, 1 Mg C for carbon emissions, 1 MW for fire radiative power) per year. Solid lines indicate the best least-squares fit to $\log[f(x)] = -\beta \log[x] + \log\alpha$, with the coefficient of determination r^2. The coefficients α and β were derived from liner regression in log–log space.

expansion often escape containment, particularly during extreme drought years, and may spread into adjacent degraded forest areas (Libonati *et al* 2022). This overlap between human and lightning ignition susceptibility can lead to increased fire frequency, extent and severity (Jones *et al* 2024).

Besides local environmental changes, climate change is also contributing to elevated fire risk in the Brazilian Amazon by extending the dry season and altering rainfall patterns (Bottino *et al* 2024). This may result in a feedback loop in which anthropogenic disturbances, fire activity and their associated carbon emissions amplify global climate change, further intensifying fire risk in the region. Moreover, evidence suggests that fires in the Amazon alter lightning occurrence through the injection of smoke into the atmosphere, which in turn alters cloud microphysical processes and, consequently, thunderstorm electrification (Fernandes *et al* 2006, Pinto Neto *et al* 2023). Future research should not only account for the potential increase in lightning-ignited fires driven by more frequent droughts associated with climate and deforestation (Bekenshtein *et al* 2023), but also further explore the interactions and feedback between anthropogenic and lightning ignitions, particularly in regions where they co-occur, to better capture compound fire dynamics.

4.2. Potential influence of ENSO on lightning fires

Although the limited length of our study period prevented a comprehensive analysis of ENSO impacts on lightning fire dynamics, we hypothesize that ENSO phases could potentially influence lightning and fire patterns. Previous research suggests that lightning activity may increase during La Niña phases due to enhanced convective activity over parts of the Amazon (Williams *et al* 2002, Sátori *et al* 2009). However, La Niña years are also typically wetter in the Amazon, which may suppress fire occurrence despite increased lightning. Conversely, El Niño conditions are often associated with severe drought and reduced precipitation across the Amazon, potentially lowering lightning frequency but rising flammable conditions (Jacobson and Streets 2009, Clark *et al* 2017, Finney *et al* 2018, 2020). In this context, a smaller number of lightning strokes may lead to more lightning ignitions during El Niño events due to a higher lightning ignition efficiency (Hessilt *et al* 2022, Coogan *et al* 2025). During our study period, La Niña conditions prevailed during 2020–2022 followed by a moderately strong El Niño in 2023–2024. Our analysis showed lower numbers of lightning-ignited fires during the La Niña phase compared to the El Niño phase (figure 4(a)). The 2023–2024 El Niño event, combined with other climatic factors that intensified the severity and duration of drought (Espinoza *et al* 2024), was associated with nearly a twofold increase in lightning fires in 2024 (a total of 558 vs 288 in 2022). These ignitions occurred throughout the fire season, peaking in September and October (figure 4(d)), indicating a persistent climatic driver rather than isolated weather events. While these observations may be too anecdotal to draw strong conclusions, they underscore the possibility of interactions between ENSO phases, lightning activity, and fire dynamics. The relatively short time series limits our ability to draw further conclusions on relationships between ENSO phases, lightning activity, and fire dynamics. Longer-term records of fire ignition attribution are needed to better quantify the influence of ENSO on lightning fire regimes across the Amazon (Goodman *et al* 2000, Hamid *et al* 2001, Yoshida *et al* 2007).

4.3. Limitations

While our study confirms the occurrence of some lightning-ignited fires in the Brazilian Amazon, considerable uncertainty remains in the attribution at large spatial scales. One key limitation stems from the spatial and temporal resolutions in satellite fire products, which can result in many fire events observed in the reference dataset going undetected, especially those of smaller size or shorter duration. Lightning-ignited fires in this region may often be low-intensity understory fires, making them more difficult to detect than the high-intensity fires typically associated with anthropogenic deforestation. In our study, we were unable to match 13 ground-verified lightning fires with fire events from the AFD. Hence, a relevant proportion of lightning fires in the region might be undetected in the AFD.

In addition, the imbalance between lightning and anthropogenic fires posed limitations on defining the threshold criteria and comparing ignition probabilities between the two fire types with equal confidence, and inevitably constrained the overall precision of the attribution. Moreover, even when lightning fire events were detected by satellites, some of them could not be matched with lightning strokes within the defined spatial and temporal windows. This mismatch introduces further attribution uncertainty and may be related to several factors, including the spatiotemporal resolution of remotely sensed fire data (Moris *et al* 2023), the detection efficiency of the lightning detection systems (Said and Murphy 2016), and the spatiotemporal limits applied to match fire and lightning data (Moris *et al* 2020).

5. Conclusions

Our study presents the first assessment of the spatio-temporal distribution of lightning fires in the Brazilian Amazon. Our findings suggest that lightning fires accounted for 0.2%–0.4% of all fires and 1.1%–1.3% of the total burned area between 2019 and 2024. Fire clusters with a higher lightning contribution (over 25% within a grid cell) were spatially concentrated in parts of the states of Pará, Amazonas, and Rondônia. Lightning-ignited and human-ignited fires exhibited comparable seasonal patterns, peaking in the dry season between September and October. As lightning occurs mostly in concurrence with heavy rainfall during thunderstorms, we found that lightning ignitions generally occur under wetter climatic conditions compared to human ignitions. Furthermore, compared to human-ignited fires, lightning-ignited fires constituted rare, large-scale, and high-intensity events. Although lightning-ignited fires account for only a small fraction of the total number of fires in the Brazilian Amazon, our results provide the first quantitative evidence of their existence, the environmental conditions surrounding their occurrence, their behavior and their possibly important role in shaping local fire dynamics in remote tropical forest regions.

Data availability statement

The remotely sensed fire data from https://zenodo.org/records/14338495, https://ladsweb.modaps.eosdis.nasa.gov/archive/allData/5200/VNP14IMG/; Lightning data is available in gridded format upon reasonable request; Land cover and infrastructure data from https://brasil.mapbiomas.org/downloads/, https://download.geofabrik.de/; https://brasil.mapbiomas.org/downloads/ https://download.geofabrik.de/; Meteorological data from https://cds.climate.copernicus.eu/datasets/reanalysis-era5-land?tab=download; Ground reference data on the cause is available upon request.

Supplementary material available at https://doi.org/10.1088/1748-9326/ae3786/data1.

Acknowledgments

Cunhui Zhang would like to thank the China Scholarship Council (CSC) for funding her study in the Netherlands. JVM acknowledges the funding from the European Union's Horizon Europe research and innovation programme under the Marie Sklodowska-Curie Grant Agreement No. 10114741.

Conflict of interest

The authors declare no competing interests.

Author contributions

Cunhui Zhang 0009-0002-5072-5926
Conceptualization (equal), Data curation (equal), Formal analysis (equal), Methodology (equal), Validation (equal), Visualization (equal), Writing – original draft (equal), Writing – review & editing (equal)

Thomas A J Janssen 0000-0002-6325-8039
Data curation (equal), Methodology (equal), Supervision (equal), Writing – review & editing (equal)

Jose V Moris 0000-0003-0241-7910
Methodology (equal), Supervision (equal), Writing – review & editing (equal)

Niels Andela 0000-0002-8241-6143
Resources (supporting), Writing – review & editing (equal)

Matthew W Jones 0000-0003-3480-7980
Resources (equal), Writing – review & editing (equal)

Renata Libonati 0000-0001-7570-1993
Validation (equal), Writing – review & editing (equal)

Lucas Menezes 0000-0003-1016-8846
Data curation (equal)

Imma Oliveras Menor 0000-0001-5345-2236
Writing – review & editing (equal)

Carlota Segura-Garcia 0009-0001-8749-8360
Writing – review & editing (equal)

Sander Veraverbeke 0000-0003-1362-5125
Conceptualization (equal), Formal analysis (equal), Methodology (equal), Supervision (equal), Visualization (equal), Writing – review & editing (equal)

References

Alencar A A, Brando P M, Asner G P and Putz F E 2015 Landscape fragmentation, severe drought, and the new Amazon forest fire regime *Ecol. Appl.* **25** 1493–505

Almeida A C, Rocha B R P, Souza J R S, Sá J A S and Filho J A P 2012 Cloud-to-ground lightning observations over the eastern Amazon Region *Atmos. Res.* **117** 86–90

Almeida C T, Oliveira-Júnior J F, Delgado R C, Cubo P and Ramos M C 2017 Spatiotemporal rainfall and temperature trends throughout the Brazilian Legal Amazon, 1973–2013 *Int. J. Climatol.* **37** 2013–26

Andela N, Morton D C, Schroeder W, Chen Y, Brando P M and Randerson J T 2022 Tracking and classifying Amazon fire events in near real time *Sci. Adv.* **8** eabd2713

Aragão L E O C, Poulter B, Barlow J B, Anderson L O, Malhi Y, Saatchi S, Phillips O L and Gloor E 2014 Environmental change and the carbon balance of Amazonian forests *Biol. Rev.* **89** 913–31

Bekenshtein R, Price C and Mareev E 2023 Is Amazon deforestation decreasing the number of thunderstorms over South America? *Q. J. R. Meteorol. Soc.* **149** 2514–26

Bottino M J, Nobre P, Giarolla E, da Silva Junior M B, Capistrano V B, Malagutti M, Tamaoki J N, de Oliveira B F A and Nobre C A 2024 Amazon savannization and climate change are projected to increase dry season length and temperature extremes over Brazil *Sci. Rep.* **14** 5131

Brando P M *et al* 2014 Abrupt increases in Amazonian tree mortality due to drought–fire interactions *Proc. Natl Acad. Sci.* **111** 6347–52

Brando P M, Paolucci L, Ummenhofer C C, Ordway E M, Hartmann H, Cattau M E, Rattis L, Medjibe V, Coe M T and Balch J 2019 Droughts, wildfires, and forest carbon cycling: a pantropical synthesis *Annu. Rev. Earth Planet Sci.* **47** 555–81

Bush M B, Silman M R, McMichael C and Saatchi S 2008 Fire, climate change and biodiversity in Amazonia: a Late-Holocene perspective *Phil. Trans. R. Soc. B* **363** 1795–802

Bush M, Flenley J and Gosling W 2011 *Tropical Rainforest Responses to Climatic Change* (Springer)

Cardoso D *et al* 2017 Amazon plant diversity revealed by a taxonomically verified species list *Proc. Natl Acad. Sci.* **114** 10695–700

Clark S K, Ward D S and Mahowald N M 2017 Parameterization-based uncertainty in future lightning flash density *Geophys. Res. Lett.* **44** 2893–901

Cochrane M A 2003 Fire science for rainforests *Nature* **421** 913–9

Coogan S C P, Cannon A J and Flannigan M D 2025 Lightning ignition efficiency in Canadian forests *Fire Ecol.* **21** 34

Costa D F, Gomes H B, Silva M C L and Zhou L 2022 The most extreme heat waves in Amazonia happened under extreme dryness *Clim. Dyn.* **59** 281–95

Cummins K L, Murphy M J, Bardo E A, Hiscox W L, Pyle R B and Pifer A E 1998 A combined TOA/MDF technology upgrade of the US national lightning detection network *J. Geophys. Res.* **103** 9035–44

da Silva R M D, Lopes A G and Santos C A G 2023 Deforestation and fires in the Brazilian Amazon from 2001 to 2020: impacts on rainfall variability and land surface temperature *J. Environ. Manage.* **326** 116664

DiCiccio T J and Efron B 1996 Bootstrap confidence intervals *Stat. Sci.* **11** 189–228

Dorph A, Marshall E, Parkins K A and Penman T D 2022 Modelling ignition probability for human- and lightning-caused wildfires in Victoria, Australia *Nat. Hazards Earth Syst. Sci.* **22** 3487–99

Espinoza J-C, Jimenez J C, Marengo J A, Schongart J, Ronchail J, Lavado-Casimiro W and Ribeiro J V M 2024 The new record of drought and warmth in the Amazon in 2023 related to regional and global climatic features *Sci. Rep.* **14** 8107

Fawcett T 2006 An introduction to ROC analysis *Pattern Recognit. Lett.* **27** 861–74

Fernandes W A, Pinto I R C A, Pinto O Jr, Longo K M and Freitas S R 2006 New findings about the influence of smoke from fires on the cloud-to-ground lightning characteristics in the Amazon region *Geophys. Res. Lett.* **33** L20810

Feron S, Cordero R R, Damiani A, MacDonell S, Pizarro J, Goubanova K, Valenzuela R, Wang C, Rester L and Beaulieu A 2024 South America is becoming warmer, drier, and more flammable *Commun. Earth Environ.* **5** 501

Finney D L, Doherty R M, Wild O, Stevenson D S, MacKenzie I A and Blyth A M 2018 A projected decrease in lightning under climate change *Nat. Clim. Change* **8** 210–3

Finney D L, Marsham J H, Wilkinson J M, Field P R, Blyth A M, Jackson L S, Kendon E J, Tucker S O and Stratton R A 2020 African lightning and its relation to rainfall and climate change in a convection-permitting model *Geophys. Res. Lett.* **47** e2020GL088163

Flores B M *et al* 2024 Critical transitions in the Amazon forest system *Nature* **626** 555–64

Goodman S J, Buechler D E, Knupp K, Driscoll K and McCaul E W Jr 2000 The 1997–98 El Nino event and related wintertime lightning variations in the southeastern United States *Geophys. Res. Lett.* **27** 541–4

Gora E M, Burchfield J C, Muller-Landau H C, Bitzer P M and Yanoviak S P 2020a Pantropical geography of lightning-caused disturbance and its implications for tropical forests *Glob. Change Biol.* **26** 5017–26

Gora E M, McGregor I R, Muller-landau H C, Burchfield J C, Cushman K C, Rubio V E, Mori G B, Sullivan M J P, Chmielewski M W and Esquivel-muelbert A 2025 Storms are an important driver of change in tropical forests *Ecol. Lett.* **28** e70157

Gora E M, Muller-Landau H C, Burchfield J C, Bitzer P M, Hubbell S P, Yanoviak S P and Bellingham P 2020b A mechanistic and empirically supported lightning risk model for forest trees *J. Ecol.* **108** 1956–66

Hamid E Y, Kawasaki Z and Mardiana R 2001 Impact of the 1997–98 El Niño event on lightning activity over Indonesia *Geophys. Res. Lett.* **28** 147–50

Hendricks L B, Anshari G Z and Gavin D G 2024 Fire in the rainforest: a 3200-year history of fire in a West Kalimantan, Indonesia, tropical rainforest *Ecosphere* **15** e4918

Hessilt T D, Abatzoglou J T, Chen Y, Randerson J T, Scholten R C, van der Werf G and Veraverbeke S 2022 Future increases in lightning ignition efficiency and wildfire occurrence expected from drier fuels in boreal forest ecosystems of western North America *Environ. Res. Lett.* **17** 054008

ICMBio 2025 ICMBIO amazon natural fires (available at: www.gov.br/icmbio/pt-br)

Instituto Brasileiro de Geografia e Estatística—IBGE 2024 Malha Municipal Digital e Áreas Territoriais 2024 (available at:

www.ibge.gov.br/geociencias/organizacao-do-territorio/malhas-territoriais/15774-malhas.html?=&t=acesso-ao-produto)
Jacobson M Z and Streets D G 2009 Influence of future anthropogenic emissions on climate, natural emissions, and air quality *J. Geophys. Res.* **114** D08118
Janssen T A J, Jones M W, Finney D, van der Werf G R, van Wees D, Xu W and Veraverbeke S 2023 Extratropical forests increasingly at risk due to lightning fires *Nat. Geosci.* **16** 1136–44
Janssen T, Fleischer K, Luyssaert S, Naudts K and Dolman H 2020 Drought resistance increases from the individual to the ecosystem level in highly diverse Neotropical rainforest: a meta-analysis of leaf, tree and ecosystem responses to drought *Biogeosciences* **17** 2621–45
Janssen T, van der Velde Y, Hofhansl F, Luyssaert S, Naudts K, Driessen B, Fleischer K and Dolman H 2021 Drought effects on leaf fall, leaf flushing and stem growth in the Amazon forest: reconciling remote sensing data and field observations *Biogeosciences* **18** 4445–72
Jiménez-Muñoz J C, Mattar C, Barichivich J, Santamaría-Artigas A, Takahashi K, Malhi Y, Sobrino J A and Schrier G V D 2016 Record-breaking warming and extreme drought in the Amazon rainforest during the course of El Niño 2015–2016 *Sci. Rep.* **6** 33130
Jones M W *et al* 2024 State of wildfires 2023–2024 *Earth Syst. Sci. Data* **16** 3601–85
Kapos V 1989 Effects of isolation on the water status of forest patches in the Brazilian Amazon *J. Trop. Ecol.* **5** 173–85
Keller M, Palace M, Asner G P, Pereira J R and Silva J N M 2004 Coarse woody debris in undisturbed and logged forests in the eastern Brazilian Amazon *Glob. Change Biol.* **10** 784–95
Khanna J, Medvigy D, Fueglistaler S and Walko R 2017 Regional dry-season climate changes due to three decades of Amazonian deforestation *Nat. Clim. Change* **7** 200–4
Lapola D M 2023 The drivers and impacts of Amazon forest degradation *Science* **379** eabp8622
Larjavaara M, Pennanen J and Tuomi T J 2005 Lightning that ignites forest fires in Finland *Agric. For. Meteorol.* **132** 171–80
Laurance W F, Cochrane M A, Bergen S, Fearnside P M, Delamônica P, Barber C, D'angelo S and Fernandes T 2001 The future of the Brazilian Amazon *Science* **291** 438–9
Leigh E G 1975 Structure and climate in tropical rain forest *Annu. Rev. Ecol. Syst.* **6** 67–86
Libonati R *et al* 2021 Twenty-first century droughts have not increasingly exacerbated fire season severity in the Brazilian Amazon *Sci. Rep.* **11** 4400
Libonati R *et al* 2022 Drought–heatwave nexus in Brazil and related impacts on health and fires: a comprehensive review *Ann. New York Acad. Sci.* **1517** 44–62
Liu Y, Spracklen D V, Parker D J, Holden J, Ge J and Guo W 2025 Recent forest loss in the Brazilian Amazon causes substantial reductions in dry season precipitation *AGU Adv.* **6** e2025AV001670
Longo M *et al* 2025 Degradation and deforestation increase the sensitivity of the Amazon Forest to climate extremes *Environ. Res. Lett.* **20** 054024
MapBiomas Project 2024 MapBiomas general "Handbook"—Algorithm Theoretical Basis Document (ATBD)—collection 9 10.58053/MapBiomas/ICCL5B
Marengo J A, Espinoza J-C, FU R, Jimenez Muñoz J C, Alves L M, Da Rocha H R and Schöngart J 2024 Long-term variability, extremes and changes in temperature and hydrometeorology in the Amazon region: a review *Acta Amazon* **54** e54es22098
Marengo J A, Souza C M, Thonicke K, Burton C, Halladay K, Betts R A, Alves L M and Soares W R 2018 Changes in climate and land use over the amazon region: current and future variability and trends *Front. Earth Sci.* **6** 228
Menezes L S, de Oliveira A M, Santos F L M, Russo A, de Souza R A F, Roque F O and Libonati R 2022 Lightning patterns in the Pantanal: untangling natural and anthropogenic-induced wildfires *Sci. Total Environ.* **820** 153021
Monteith J and Unsworth M 2013 *Principles of Environmental Physics: Plants, Animals, and the Atmosphere* (Academic)
Moreira D *et al* 2025 Widespread and exceptional reduction in river water levels across the Amazon basin during the 2023 extreme drought revealed by satellite altimetry and SWOT *Geophys. Res. Lett.* **52** e2025GL116180
Moris J V *et al* 2023 A global database on holdover time of lightning-ignited wildfires *Earth Syst. Sci. Data* **15** 1151–63
Moris J V, Ascoli D and Hunt H G P 2024a Survival functions of holdover time of lightning-ignited wildfires *Electr. Power Syst. Res.* **231** 110296
Moris J V, Ascoli D and Hunt H G P 2024b A new method to assess the probability of lightning causing wildfires (available at: https://ieeexplore.ieee.org/abstract/document/10832489)
Moris J V, Conedera M, Nisi L, Bernardi M, Cesti G and Pezzatti G B 2020 Lightning-caused fires in the Alps: identifying the igniting strokes *Agric. For. Meteorol.* **290** 107990
Moura M M *et al* 2019 Relation of El Niño and La Niña phenomena to precipitation, evapotranspiration and temperature in the Amazon basin *Sci. Total Environ.* **651** 1639–51
Muñoz-Sabater J *et al* 2021 ERA5-Land: a state-of-the-art global reanalysis dataset for land applications *Earth Syst. Sci. Data* **13** 4349–83
Nobre C A, Sampaio G, Borma L S, Castilla-Rubio J C, Silva J S and Cardoso M 2016 Land-use and climate change risks in the Amazon and the need of a novel sustainable development paradigm *Proc. Natl Acad. Sci.* **113** 10759–68
OpenStreetMap 2021 OpenStreetMap (available at: www.openstreetmap.org/copyright)
Otto Tetens 1930 *Über_einige_meteorologische_Begriffe* (Friedrich Vieweg & Sohn Akt.- Gesellschaft)
Pinto I and Pinto O Jr 2003 Cloud-to-ground lightning distribution in Brazil *J. Atmos. Sol.-Terr. Phys.* **65** 733–7
Pinto Neto O, Pinto I R C A, Pinto Junior O and Williams E R 2023 Evidence of a link between Amazon fires and lightning *J. Atmos. Sol.-Terr. Phys.* **249** 106095
Pivello V R *et al* 2021 Understanding Brazil's catastrophic fires: causes, consequences and policy needed to prevent future tragedies *Perspect. Ecol. Conserv.* **19** 233–55
Ray D, Nepstad D and Moutinho P 2005 Micrometeorological and canopy controls of fire susceptibility in a forested Amazon landscape *Ecol. Appl.* **15** 1664–78
Said R K, Inan U S and Cummins K L 2010 Long-range lightning geolocation using a VLF radio atmospheric waveform bank *J. Geophys. Res.* **115** D23108
Said R and Murphy M 2016 GLD360 upgrade: performance analysis and applications
Sampaio G, Nobre C, Costa M H, Satyamurty P, Soares-Filho B S and Cardoso M 2007 Regional climate change over eastern Amazonia caused by pasture and soybean cropland expansion *Geophys. Res. Lett.* **34** L17709
Sátori G, Williams E and Lemperger I 2009 Variability of global lightning activity on the ENSO time scale *Atmos. Res.* **91** 500–7
Schmidt I B and Eloy L 2020 Fire regime in the Brazilian Savanna: recent changes, policy and management *Flora* **268** 151613
Schroeder W, Oliva P, Giglio L and Csiszar I A 2014 The New VIIRS 375 m active fire detection data product: algorithm description and initial assessment *Remote Sens. Environ.* **143** 85–96
Silveira M V F, Silva-Junior C H L, Anderson L O, Aragão L E O C and Silveira M V F 2022 Amazon fires in the 21st century: the year of 2020 in evidence *Glob. Ecol. Biogeogr.* **31** 2026–40
Singh J, Ashfaq M, Skinner C B, Anderson W B, Mishra V and Singh D 2022 Enhanced risk of concurrent regional droughts with increased ENSO variability and warming *Nat. Clim. Change* **12** 163–70

Sombroek W 2001 Spatial and temporal patterns of Amazon rainfall *AMBIO: J. Hum. Environ.* **30** 388–96

Souza C M Jr *et al* 2020 Reconstructing three decades of land use and land cover changes in Brazilian biomes with Landsat archive and earth engine *Remote Sens.* **12** 2735

Spracklen D V and Garcia-Carreras L 2015 The impact of Amazonian deforestation on Amazon basin rainfall *Geophys. Res. Lett.* **42** 9546–52

The Brazilian National Transport Department 2024 the Brazilian national transport department (available at: www.gov.br/dnit/pt-br)

Thonicke K, Venevsky S, Sitch S and Cramer W 2001 The role of fire disturbance for global vegetation dynamics: coupling fire into a Dynamic Global Vegetation Model *Glob. Ecol. Biogeogr.* **10** 661–77

Uhl C and Kauffman J B 1990a Deforestation, fire susceptibility, and potential tree responses to fire in the eastern Amazon *Ecology* **71** 437–49

Veraverbeke S, Janssen T A J, Brambleby E, Jones M, Zoletto B and van der Sande M T 2025 Lightning impacts on global forest and carbon dynamics: current understanding and knowledge gaps *Glob. Change Biol.* **31** e70179

Williams E *et al* 2002 Contrasting convective regimes over the Amazon: implications for cloud electrification *J. Geophys. Res.* **107** LBA–50

Xu W, Scholten R C, Hessilt T D, Liu Y and Veraverbeke S 2022 Overwintering fires rising in eastern Siberia *Environ. Res. Lett.* **17** 45005

Yanoviak S P, Gora E M, Bitzer P M, Burchfield J C, Muller-Landau H C, Detto M, Paton S and Hubbell S P 2020 Lightning is a major cause of large tree mortality in a lowland neotropical forest *New Phytol.* **225** 1936–44

Yoon J-H and Zeng N 2010 An Atlantic influence on Amazon rainfall *Clim. Dyn.* **34** 249–64

Yoshida S, Morimoto T, Ushio T and Kawasaki Z 2007 ENSO and convective activities in Southeast Asia and western Pacific *Geophys. Res. Lett.* **34** L21806

Zhao L, Dai A and Dong B 2018 Changes in global vegetation activity and its driving factors during 1982–2013 *Agric. For. Meteorol.* **249** 198–209